

# Rubberised concrete confined with thin-walled steel profiles: a ductile composite for building structures.

JAFARIFAR, N., BAGHERI SABBAGH, A. and UCHEHARA, I.

2023



# Rubberised concrete confined with thin-walled steel profiles; a ductile composite for building structures

Naeimeh Jafarifar<sup>a</sup>, Alireza Bagheri Sabbagh<sup>b</sup>, Ikechukwu Uchehara<sup>a</sup>

<sup>a</sup> School of Architecture and Built Environment, Robert Gordon University, Scotland, UK

<sup>b</sup> School of Engineering, University of Aberdeen, Scotland, UK

## ARTICLE INFO

### Keywords:

Cold-formed steel  
Rubberised concrete  
Composite structures  
Ductility  
Low-carbon structures

## ABSTRACT

Tyre components are high-quality materials, which can be utilised and disposed into construction projects. Despite its high ductility and impact resistance, rubberised concrete (RuC) with high rubber content has a strength much lower than that of conventional concrete. Previous research shows that confinement by a jacket material can significantly improve the strength of RuC. This paper presents how infilling RuC to cold-formed steel (CFS) sections improves strength of RuC and local-buckling-resistance of CFS thin-walled sections, resulting composite elements where the advantage of each material cancels out the disadvantage of another. In this research, the composite RuC-CFS elements are developed and tested with the purpose of using them for structural frames with high energy dissipation capacity under extreme loading conditions, while providing resource-efficiency by using lightweight CFS and recycled RuC materials. To enable infilling long steel hollow sections for beams and columns, the experimental RuC mixes are designed for self-compaction (SCC). The results reveal that 35 % rubber content (by volume) and 3 mm thickness of the CFS profile (S275 grade) gives the best performance of the composite by adding 19 % to the capacity of the individual constituent materials.

## 1. Introduction

Huge quantities of used tyres are a threat to the environment being extremely durable and non-biodegradable. Tyre components, including rubber, high-strength steel cord, wire and textile, are high-quality materials, which can be utilised and disposed into construction projects [15,16,1,23]. Extensive research has been carried out in the past two decades, for using crumb rubber or various size rubber particles as a replacement for mineral aggregates in concrete [1,23,14,24,27,21,10,9,12,13,25,11].

Using rubber aggregate in concrete can enhance its ductility, impact resistance, and energy absorption, although high amounts of rubber (more than 20 %) can negatively affect the strength properties of RuC [23,14]. This can be due to lower stiffness of rubber aggregate compared to mineral aggregates or due to poor adhesion between rubber and cement binder. Replacement of mineral aggregates in concrete with high rubber contents (replacement volumes greater than 50–60 %) may result in a compressive strength much lower (up to 90 %) than that of conventional concrete. However, studies show that confinement of RuC by a

jacket material significantly improves compressive strength of RuC to a level suitable for structural applications. Highly confined rubberised concrete can lead to high-strength and highly deformable concrete elements and structures [24]. Various materials have been used for confining RuC, including fibre reinforced polymer (FRP) jackets [27], glass FRP (GFRP) pipes [21], and cold-formed steel (CFS) tubes [10,9,12,13,25].

Compared to conventional hot-rolled sections, CFS is more resource-efficient, less expensive to manufacture, and of a greater flexibility for production. The load-bearing capacity of non-composite CFS frame structures is normally dominated by premature local/distortional buckling of their thin-walled sectional elements [4,5,26,22]. This inhibits fast uptake of CFS framed structures, especially in multi-storey construction. Infilling RuC to CFS hollow sections, apart from improving the strength properties of RuC through confinement, has the additional benefit of restraining CFS and delaying its premature local buckling failure. This increases the load bearing capacity of these composite elements. The high ductility of RuC is very compatible with steel deformability, and the energy absorption capacity of the composite

**Abbreviations:** RuC, Rubberised Concrete; CFS, Cold-Formed Steel; SCC, Self-Compacting Concrete; RuC-CFS, Rubberised Concrete infilled into Cold-Formed Steel profile; FRP, Fibre Reinforced Polymer; GFRP, Glass Fibre Reinforced Polymer; RuSCC, Rubberised Self-Compacting Concrete; RCC, Roller-Compacted Concrete; RuRCC, Rubberised Roller-Compacted Concrete.

**E-mail addresses:** [n.jafarifar@rgu.ac.uk](mailto:n.jafarifar@rgu.ac.uk) (N. Jafarifar), [alireza.bsabbagh@abdn.ac.uk](mailto:alireza.bsabbagh@abdn.ac.uk) (A. Bagheri Sabbagh), [i.uchehara@rgu.ac.uk](mailto:i.uchehara@rgu.ac.uk) (I. Uchehara).

<https://doi.org/10.1016/j.istruc.2023.01.134>

Received 10 August 2022; Received in revised form 1 January 2023; Accepted 25 January 2023

Available online 9 February 2023

2352-0124/© 2023 The Authors. Published by Elsevier Ltd on behalf of Institution of Structural Engineers. This is an open access article under the CC BY license (<http://creativecommons.org/licenses/by/4.0/>).

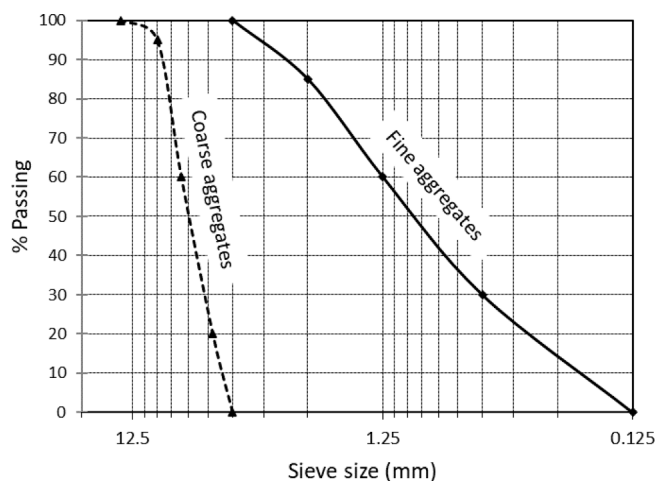


Fig. 1. Grading of the course and fine mineral aggregates in the reference mix.

**Table 1**  
Grading of the course and fine mineral aggregates in the reference mix.

Coarse Aggregates		Fine Aggregates	
Sieve Diameter (mm)	Passing	Sieve Diameter (mm)	Passing
5.00	0 %	0.125	0 %
6.00	20 %	0.5	30 %
8.00	60 %	1.25	60 %
10.00	95 %	2.5	85 %
14.00	100 %	5	100 %

is significantly larger than the sum of its values for the individual non-composite components [10,12]. These composite elements can, therefore, be used where a high energy dissipation and ductility capacities are sought (e.g., in earthquake-prone areas) [9,13,25]. In this research, the mechanical properties of these composite elements were studied for potential structural applications, including multi-storey frame construction.

Vibration of RuC infilled to hollow CFS sections as the casing of beams and columns can be practically hard or impossible. At the connection zones, where a number of bolts exist, RuC should uniformly fill in all voids and spaces around the bolts to achieve a good composite action. To enable infilling the CFS hollow sections with no void and improve the structural integrity of the composite elements, the RuC mixes need to have high workability. Therefore, self-compacting concrete (SCC) seems to be the right technology for this application, enabling easy pouring of RuC into the CFS sections. The flowable SCC can consolidate under its own weight and maintain homogeneity throughout the length of elements and in the congested zones around the bolted connections, without the need for any compaction.

For that purpose, self-compacting RuC (RuSCC) mixes were developed and studied for various percentages of rubber aggregates (35 %, 50 %, and 75 %). The workability and fresh properties of the RuSCC mixes were measured and optimised. The composite samples were cast, through infilling the RuSCC into CFS with various sectional specifications (circular and square sections, 1.6 mm and 3 mm thicknesses), and tested under compressive load. Comparative studies were carried out to investigate the level of improvement in the mechanical properties of the composite sections.

**2. Experimental programme**

Adding a high amount of rubber to concrete reduces the workability of the mix, significantly. Hence, designing RuSCC with a high rubber content, while maintaining good properties of the mix at the hardened and fresh state, is challenging and needs to be studied. For that purpose,

three different percentages (35 %, 50 %, 75 %) for the replacement of mineral aggregates with rubber aggregates were examined, as well as a reference mix with no rubber (a conventional SCC mix). The mixes were developed, and the specimens were cast and tested under confined and un-confined conditions. The confinement was achieved with CFS casings of circular and square sections made of two different types of steel and two main thicknesses, based on availability and for comparison purposes. The CFS sections had an internal dimension of 100 mm, and a length of 300 mm. Shear studs were used for some specimens (8 self-drill screws 5 × 25 mm at four sides and two levels), to see how this can affect the bond between the CFS casing and RuSCC infill. The RuSCC mixes were tested for workability at the fresh state of the mix, while the hardened specimens were tested for compressive strength. The observations and the test result are given in the following sections.

To develop the RuSCC mixes, the following steps were taken:

- Step 1: Sieving coarse and fine aggregates (both mineral aggregates and rubber aggregates)
- Step 2: Measuring particle density of aggregates
- Step 3: Casting trial RuSCC mixes (with 0 %, 35 %, 50 %, and 75 % rubber replacement) targeting no visual segregation, and a slump in the standard range of 630 ± 30 mm for the proposed application (in accordance with BS EN 12350 [6])
- Step 4: Adjusting the mix designs to improve the initial fresh properties
- Step 5: Casting the specimens with the optimised mix design for each percentage
- Step 6: Curing the specimens for 90 days
- Step 7: Grinding/capping the specimen surfaces
- Step 8: Testing the specimens using a compression machine with a 600 kN-capacity load cell, and in accordance with BS EN 12390 [7]

**2.1. Mix proportions, materials, and mixing process**

There is no standard method for SCC mix design; research institutions or construction industries normally develop their own mix proportioning method. For the purpose of this study, the reference SCC mix was developed using the guidance of BS EN 12350 [6].

Natural general purpose Tarmac Gravel Pea Shingle Product was used as mineral coarse aggregate. The bulk density of this type of aggregates was 2600 kg/m<sup>3</sup>. A blend of Kiln-dried paving sand and Jewson sharp sand was used to provide fine natural aggregates in the size range of 0.125–5 mm. The bulk density of the mixed sand before sieving was 2650 kg/m<sup>3</sup>. The mineral aggregates were washed, dried, and sieved, using laboratory sieves of square aperture of 0.125, 0.25, 0.5, 1.25, 2.5, 5.0, 10.0, and 14.0 mm, to achieve the grading curves presented in Fig. 1.

The passing percentages for the coarse and fine aggregates in these grading curves are given in Table 1. The maximum size of the coarse mineral aggregate was 14 mm.

SCC mix designs normally use volume as a key parameter because of the importance of the need to overfill the voids between the aggregate particles [6]. The absolute volume of coarse aggregates per volume of concrete was 0.3. The volume ratio of fine to coarse aggregates was chosen to be 58/43 for SCC, and the volume of fine aggregate was 57 % of the total aggregate volume. That is because, the paste is the vehicle for the transport of aggregate in SCC. So, the fine to coarse aggregate ratio in the mix was increased such that the individual coarse aggregate particles can be coated and lubricated by a layer of mortar [6].

A high strength, CEM I 52,5N Portland Cement was used offering consistent strength and compatibility with admixtures such as air-entraining agents and workability aids. This cement is suitable to be used with pozzolanic additions as cement replacement materials, such as fly-ash and silica fume. These additions can improve and maintain the segregation resistance of SCC and to reduce sensitivity to changes in

**Table 2**  
Mix design of the reference mix (Plain SCC with no rubber) and the RuSCC mixes incorporating 35%, 50% and 75% rubber by volume

Mix Constitutes	Plain SCC	RuSCC35%	RuSCC50%	RuSCC75%
Coarse mineral, 5–14 mm (kg/m <sup>3</sup> )	720	468	360	180
Coarse rubber, 5–10 mm (kg/m <sup>3</sup> )	0	95	136	204
Fine mineral, 0.15–5 mm (kg/m <sup>3</sup> )	960	624	480	240
Fine rubber, 0.15–5 mm (kg/m <sup>3</sup> )	0	128	182	273
Cement (kg/m <sup>3</sup> )	350	350	350	350
Fly Ash (kg/m <sup>3</sup> )	150	150	150	150
Water (kg/m <sup>3</sup> )	210	210	210	210
Silica Fume (kg/m <sup>3</sup> )	4	4	4	4
Superplasticiser (kg/m <sup>3</sup> )	8	11	13	15
VMA (kg/m <sup>3</sup> )	3	3	3	3
AEA (kg/m <sup>3</sup> )	2	2	2	2
Water/Powder	0.42	0.42	0.42	0.42



Fig. 2. Graded rubber and mineral aggregates prepared for a RuSCC mix.

water content [6]. Fly ash is a waste by-product from power plants (known in the UK as pulverized-fuel ash or PFA) and can further reduce the embodied carbon of the RuSCC mixes. For this study 30 % of the total cementitious material was replaced with fly ash (Cemex FLY ASH 450-N, Specification: BS EN 450–1 [8]).

The water content recommended by BS EN 12350 [6] for SCC is in the range of 160 to 185 kg per cubic meter of concrete, but based on the initial observations in this study, this amount of water does not give the required flowability to RuSCC, where a high percentage of mineral aggregate is replaced with rubber aggregate. Therefore, the water content for all mixes, including the reference mix was increased to 210 kg per cubic meter of the mix to enable comparison. With this increased

amount of water, the water to powder ratio was set at 0.42. Particle size fractions of less than 0.125 mm are considered as powder, which in this case is composed of cement, fly ash and silica fume, the amount of each is given in Table 2.

To help reduce segregation and sensitivity of the SCC (and RuSCC) mixes to change of water and powder content, the combined effects of a viscosity agent (VMA) and an air-entraining agent (AEA) was adopted using 3.0 kg/m<sup>3</sup> VMA (MasterMatrix SDC 150) and 2.0 L/m<sup>3</sup> AEA (MasterAir 119) produced by BASF [17,19]. To achieve the standard workability required for the application aimed by this research, superplasticiser (MasterGlenium SKY 1966) produced by BASF [18] was used for the given amount in Table 2 (by weight per cubic meter of concrete), depending on the amount of rubber replacement for each mix.

For the RuSCC mixes a volume percentage of fine and coarse aggregate particles from each size was replaced with rubber aggregate of the same size. RuSCC35%, RuSCC50%, and RuSCC75% denote the replacement ratios of 35 %, 50 % and 75 % (by volume) of rubber particles to mineral aggregates in the mix, respectively. The maximum size of rubber aggregates in this study is 10 mm (due to availability). Therefore, size 5–10 mm of rubber particles was used to replace the coarse mineral aggregates. Crumb rubber graded into four sizes (0.125–0.5 mm, 0.5–1.25 mm, 1.25–2.5 mm, and 2.5–5 mm) was used to replace the fine aggregates (or the natural sand) in the concrete mixes for the given volumetric percentages (Fig. 2).

All dry mix components, including all aggregates and powders, were first mixed for 2 mins before gradually adding water, plus superplasticiser (SP). Mixing then continued for 3 mins, where 25 % of the water and SP plus air entrainer was added (for optimum, consistent performance, the air-entraining admixture was dispensed with the initial batch water). Then, 50 % of water and SP was added and mixed for 6 mins. The remaining 25 % of water, SP plus VMA was then added and mixed until reaching a homogenous mix. The total mixing time required to reach a homogeneous and workable mix varied between 12mins and 40mins depending on the amount of rubber replacement. See Table 2 for mix design of the reference mix (Plain SCC) and the RuSCC mixes.

### 2.2. Fresh properties of the mixes

The flowability of RuSCC was measured using a standard slump-flow test [6], and segregation resistance was evaluated using a standard T<sub>500</sub> value method [6], as well as visual control of the concrete spread. Slump-flow test is a sensitive test for all SCC as a primary check of consistency. Visual observation and T<sub>500</sub> time can give additional information on segregation resistance and uniformity.

The observation shows that by increasing the mixing time, workability of the mixes improves and T<sub>500</sub> decreases. The mixing time required for RuSCC mixes to achieve the intended slump of 630 ± 30 mm is much longer than the time required for a conventional SCC (with no rubber). That can be attributed to the time required for rubber particles to absorb water and stabilise the consistency of the fresh mix. At



Fig. 3. Mixing stages for RuSCC.

**Table 3**  
Fresh properties of the reference mix (Plain SCC with no rubber) and the RuSCC mixes incorporating 35%, 50% and 75% rubber by volume.

Mix Constitutes	Plain SCC	RuSCC35%	RuSCC50%	RuC75%
Mixing time (mins)	12	20	35	40
T500 (s)	6.7	6.5	8	Static
Slump ave. diameter (mm)	670	630	585	Not workable
Density of the mix (kg/m <sup>3</sup> )	2373	2010	1862	1598
Any observed segregation	No	No	No	No

the mid stage of mixing for the RuSCC mixes, balling or formation of concrete ‘meatballs’ is very likely to happen (See Fig. 3, image No. 2). Adding the last proportion of water and a longer mixing time help the balls to disappear gradually and the concrete mix to achieve the expected uniformity and flowability. If the concrete ‘meatballs’ do not disappear after adding the last proportion of water, the mix design needs to be modified in a trial-and-error process. The paste content and the amount of water/superplasticiser play an important role in this regard.

Table 3 shows the fresh properties of the reference mix (Plain SCC) and the RuSCC mixes. These fresh properties were achieved after several slump-flow measurements (see Fig. 4) on various mixes and modification of the mix design in a trial-and-error process. Visual observations did not show any sign of segregation for none of the mixes, as can be seen in Fig. 4. Incorporation of more rubber particles significantly reduces flowability, and this has resulted in increased water-to-powder

ratio (0.42) in the modified mix, which is slightly higher than the ratio recommended for a conventional SCC mix. In this study, the water-to-powder ratio is kept the same for all of the studied mixes, for comparison purposes (as it is one of the main factors affecting the strength). However, a higher amount of superplasticiser has been used for mixes with higher rubber content, to improve their flowability.

As shown in Fig. 4(e), despite all efforts on modification of the mix design for RuC75%, workability of this mix did not improve and the final mix had zero flowability. This was due to the high rubber content of the mix which doesn’t let a good consistency to be achieved. However, this mix can be suitable for applications where Roller-Compacted-Concrete (RCC) technology is used. RCC is a durable and fast construction solution for heavy duty pavements and gravity dams, where the concrete is laid by paver and then roller compacted (layer by layer) just like asphalt.

A slump test for a compacted RuC incorporating 75 % rubber aggregate was carried out in this study where the mix was poured and compacted in the slump cone using a hammer. This compacted RuC mix (RuRCC75%) had an absolute zero slump (Fig. 4(f)), suitable for RCC applications.

### 2.3. Casting specimens and confinement conditions

The specimens were cast for confined and un-confined conditions and were prepared for compressive strength test according to BS EN 12390-3 [7]. The unconfined specimens were made with cylindrical moulds of a 100 mm diameter and a 300 mm height.

The confined specimens were made using steel casings of different thicknesses (1.6 mm, 3.2 mm and 3 mm), for circular and square sections. The casings were made of two different types of steel (Structural

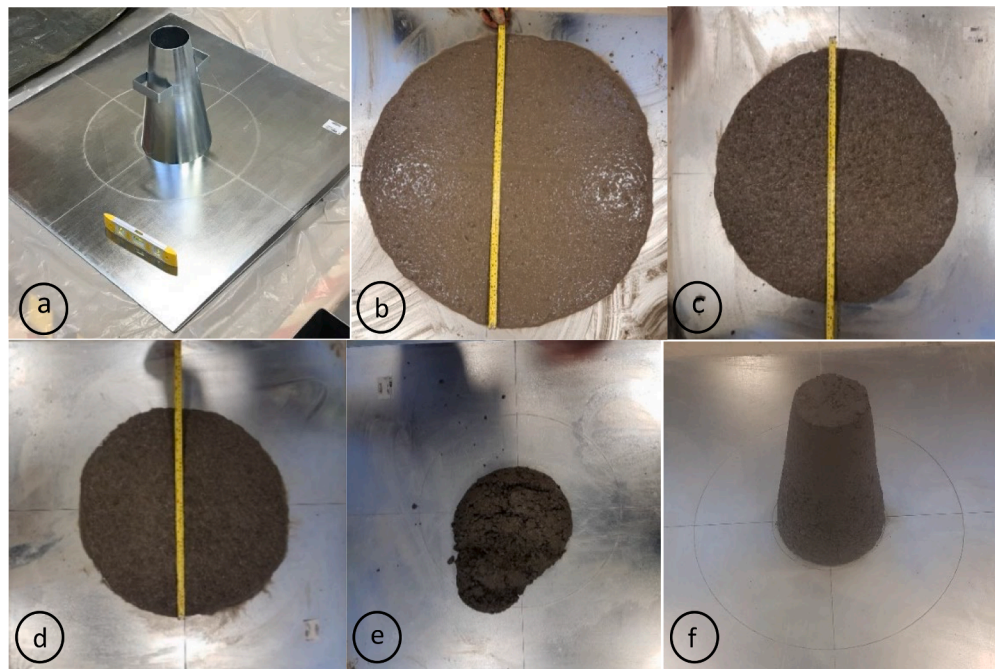


**Fig. 4.** a) slump flow measurement test, b) for the reference mix (Plain SCC); c) for RuSCC with 35% rubber, d) for RuSCC with 50% rubber, e) for RuC with 75% rubber, f) for Compacted RuC with 75% rubber (zero slump).

**Table 4**  
Specifications of the steel casings.

Specification of Casing	Steel Type	Yield Strength (MPa)	Cross Section	Outside dimension (mm)	Thickness (mm)	Net Cross-Section Area (mm <sup>2</sup> )
MS-C-1.6	Mild	220	Circular	101.6	1.6	503
MS-C-3.2	Mild	220	Circular	101.6	3.2	989
S275-S-3	S275	275	Square	100 × 100	3	1164



Fig. 5. Surface preparation/grading for the confined and unconfined specimens.

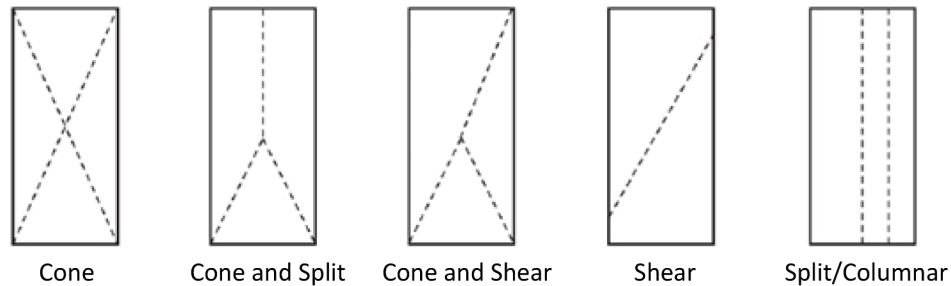


Fig. 6. Potential failure modes for cylindrical specimens under compression.



Fig. 7. Failure mode for unconfined Plain SCC cylinders (Cone failure).

Steel: S275, and Mild Steel), based on availability and for comparison purposes. S275 is a low carbon steel (less than 0.3 % carbon by weight) which is frequently used for building structures, due to high strength and toughness. Mild Steel is also a low carbon steel (in the range of 0.05 % to 0.25 % by weight) with excellent weldability, but poor corrosion resistance. CFS casings made of S275 were not available in all thicknesses required for this study. Hence, Mild Steel was used for the other thickness, to make the comparison possible. The confined specimens had a diameter of 100/101.6 mm and a length of 300 mm. The specifications of the steel casings are given in Table 4.

Shear studs were used for some of the specimens to see how this can affect the bond between the CFS casing and the RuSCC infill. This was composed of 8 self-drill screws 5 × 25 mm at four sides and two levels, inserted into the casings before concrete is poured.

Three specimens were cast from each mix (Plain SCC, RuSCC35%, RuSCC50%, and RuRCC75%) and for each confinement condition. The specimens were cured in a water tank for 90 days.

Before applying the compressive load, the surfaces of the confined and unconfined specimens were ground and prepared for testing (see Fig. 5). Thick platens of the testing machine assured uniform application

of load on the specimens.

#### 2.4. Compressive loading of specimens

The compressive loading test on the specimens was carried out in accordance with BS EN 12390–3 [7], using a 600kN INSTRON machine. The lab temperature at the time of testing was around 18 °C. The tests were carried out under load control. The loading was applied at a constant rate within the range of  $0.6 \pm 0.2$  MPa/s, with the initial load not exceeding 30 % of the expected failure load. The load–displacement curve was recorded for each specimen. For each mix/confinement condition, the average load–displacement curve for the 3 tested specimens is calculated and presented in the following section.

### 3. Results and discussion

#### 3.1. Failure mode for unconfined specimens

The failure mode of the specimens under compressive load strongly depends on the stiffness ratio between the matrix and aggregates [20].



Fig. 8. Failure mode for RuSCC35% cylinders (Shear, or Cone and Shear failure).



Fig. 9. Failure mode for RuSCC50% cylinders (Shear, Cone and Shear, or Cone and Split failure).



Fig. 10. Failure mode for RuRCC75% cylinders (mode of failure is not very clear).

For Plain SCC, a soft matrix flows around stiffer aggregates, which are natural mineral aggregates. The lateral deformation in the relatively soft matrix is larger than in the stiffer aggregates. The restraints induced by friction at the platens of the testing machine also contributes to limiting lateral expansion of the concrete specimen. This will lead to creating ‘Cones’ as the mode of failure [20], among other possible failure modes shown in Fig. 6.

Failure of Plain SCC unconfined specimens can be seen in Fig. 7. These specimens underwent a catastrophic brittle failure in a load-control setting.

For the rubberised concrete specimens, the mode of failure was very

different from what was observed for plain concrete. Fig. 8, Fig. 9 and Fig. 10 show the mode of failure for RuSCC35%, RuSCC50% and RuRCC75%, respectively. It can be seen that ‘Shear’ failure is the dominant mode of failure for those specimens although ‘Cone and Shear’ and ‘Cone and Split’ failures were also observed for some of the specimens.

Although the test for rubberised concrete specimens was also carried out in load-control, the collapse was very ductile (as opposed to catastrophic brittle failure of plain concrete specimens) and the load was sustained until a large deformation was reached beyond the peak load.

In rubberised concrete specimens, the bond between rubber

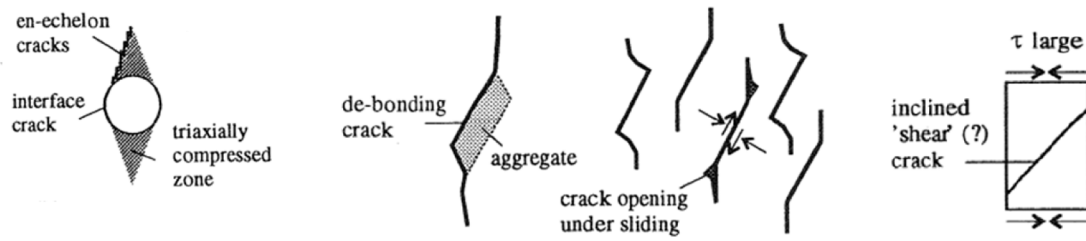


Fig. 11. The mechanical behaviour of concrete under uniaxial compression, when the bond between aggregates and cement is weak [22].

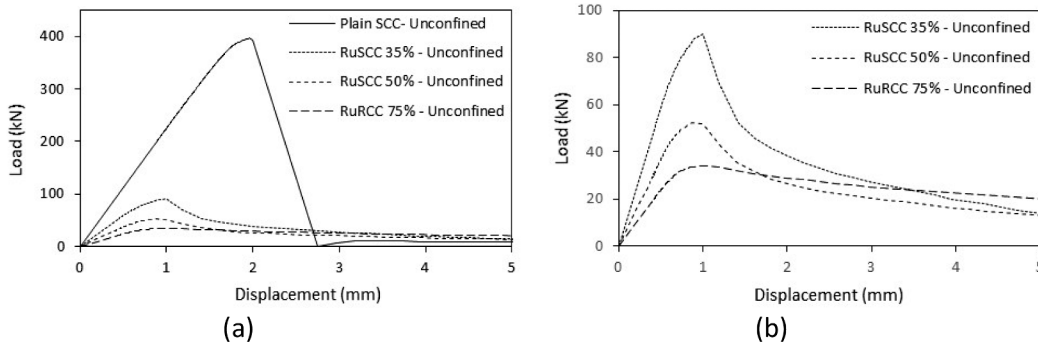


Fig. 12. Compressive strength of unconfined specimens a) All; b) Zoomed-in for rubberised concrete mixes.



Fig. 13. A) ductile failure of RuSCC-CFS; b) RuSCC infill bouncing back after unloading; c) shear studs prevent RuSCC infill bouncing back after unloading.

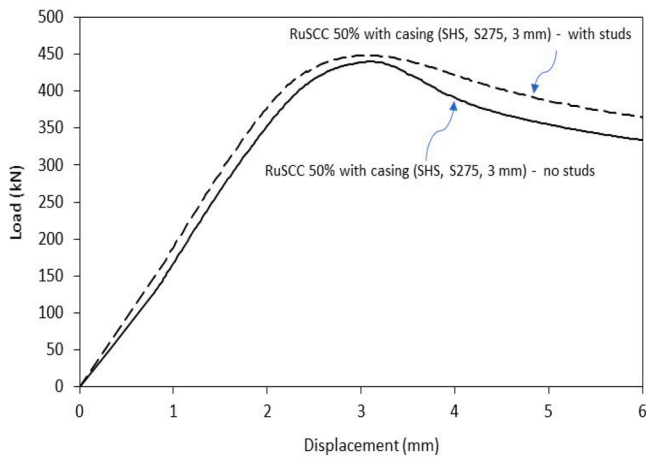


Fig. 14. Comparing the failure load for confined RuSCC50%, with and without shear studs.

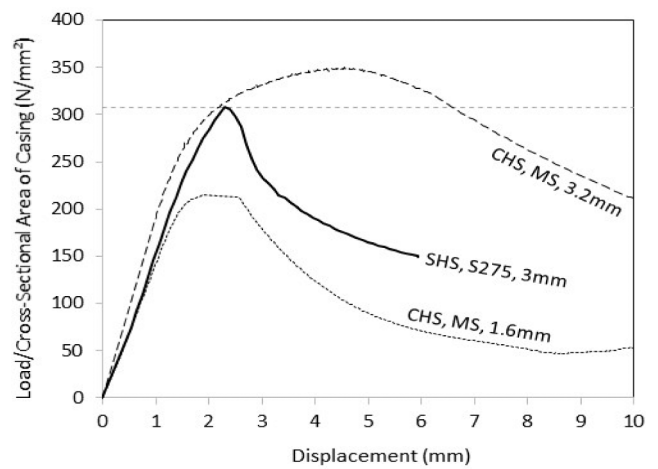


Fig. 15. Normalised load–displacement behaviour of the hollow casings (with no infill).

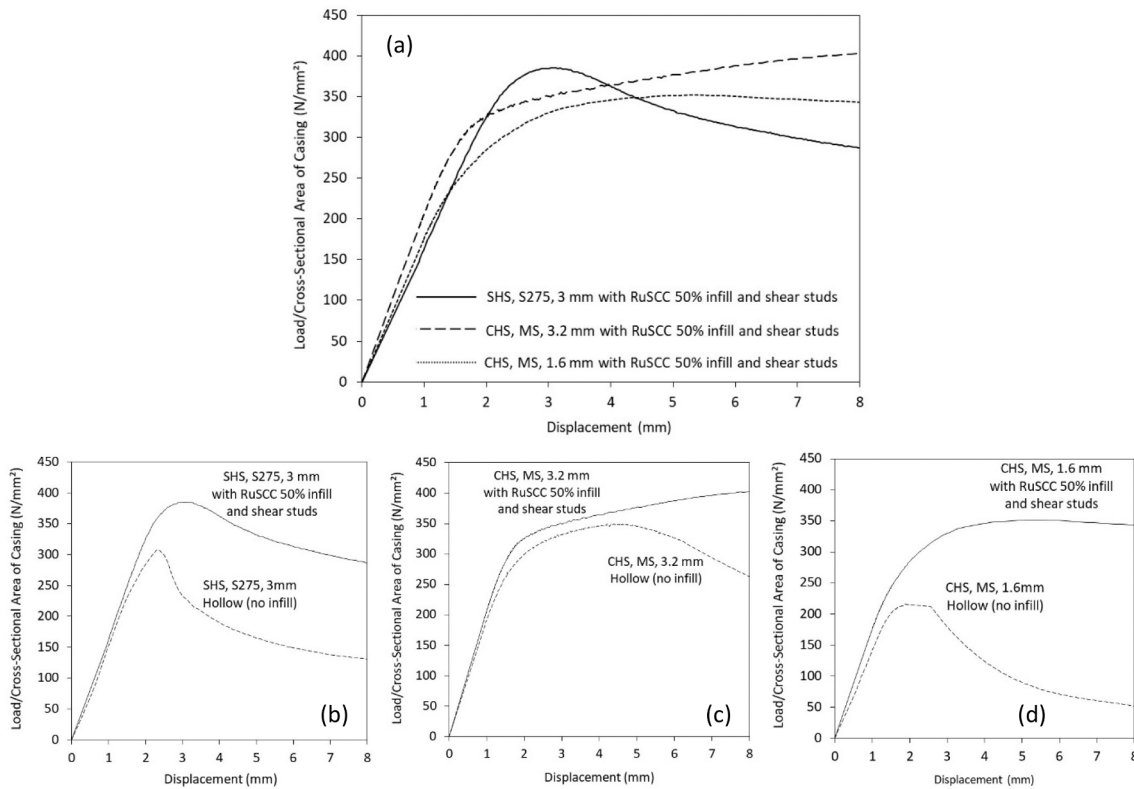


Fig. 16. Normalised load–displacement behaviour for (a) three different steel casings with infill (all composites); (b) SHS, S275, 3 mm, with and without infill; (c) CHS, MS, 3.2 mm, with and without infill; (d) CHS, MS, 1.6 mm, with and without infill.

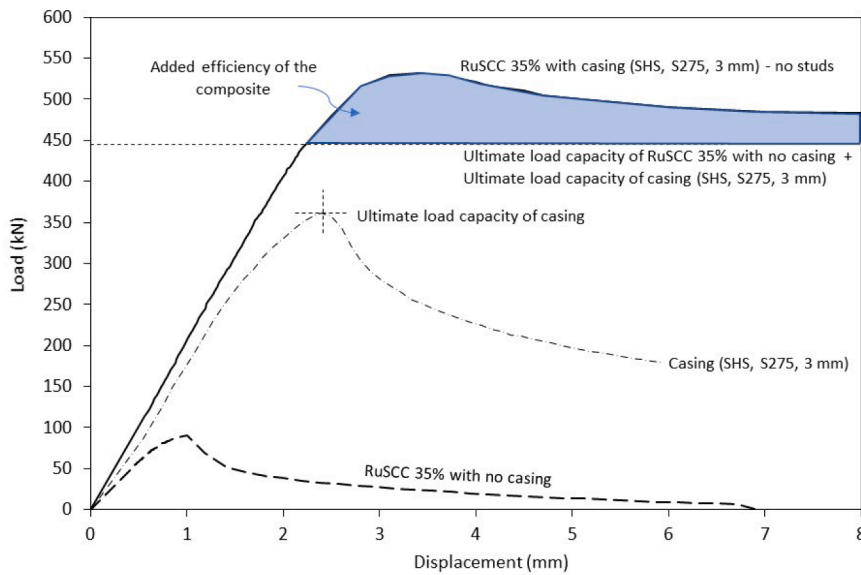


Fig. 17. The composite behaviour of RuSCC35% confined with 3 mm Structural Steel casing (SHS, S275, 3 mm).

aggregates and cement is naturally weaker than the bond between mineral aggregate and cement in a conventional plain concrete. This weak bond can cause interfacial cracks [20]. This interfacial cracks can lead to inclined shear cracks in the specimen (see Fig. 11).

Debonding cracks between rubber and cement may already develop during the hardening stage. Under compressive load, propagation of cracks under initially inclined debonding cracks or other imperfections can be responsible for the ‘Shear’ failure mode of the rubberised concrete mixes. The high deformability of rubber aggregates, which result in larger lateral expansion of the RuC specimens, can also contribute into

shear or split mode of failure. Frictional slip in cracks after the peak load and deformability of rubber aggregates make rubberised concrete an energy-absorbant material.

### 3.2. Load-Displacement behaviour for unconfined specimens

The load–displacement behaviour of the unconfined rubberised concrete specimens, for various rubber percentages, and for the reference plain concrete mix are shown in Fig. 12. This figure shows that if rubber is incorporated into concrete, the compressive strength of the

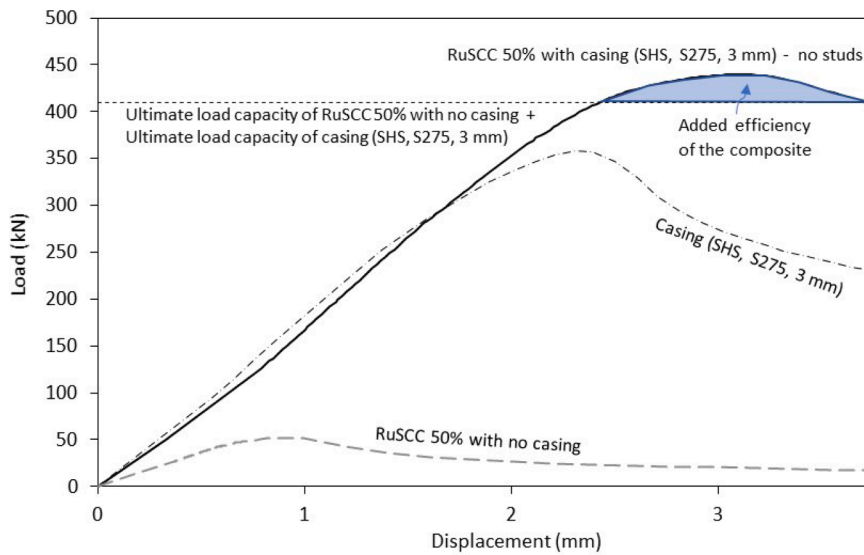


Fig. 18. The composite behaviour of RuSCC50% confined with 3 mm Structural Steel casing (SHS, S275, 3 mm).

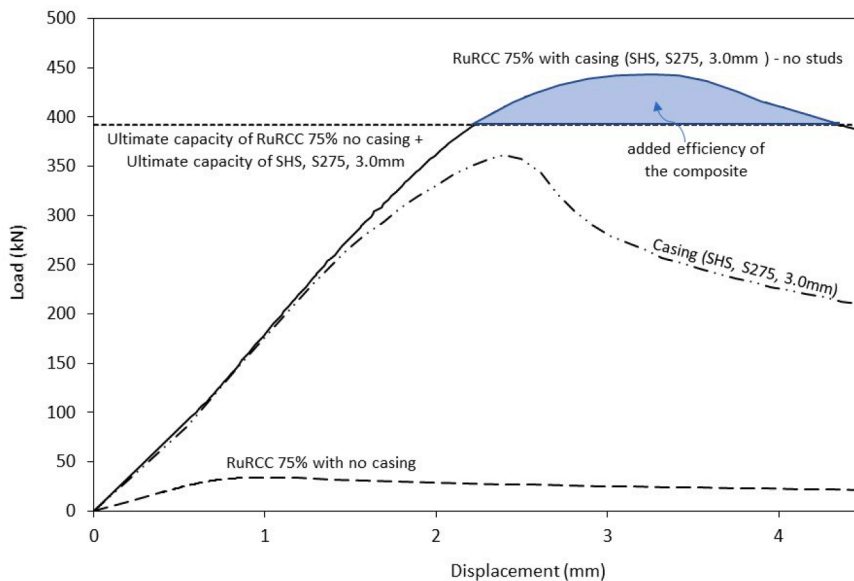


Fig. 19. The composite behaviour of RuRCC75% confined with 3 mm Structural Steel casing (SHS, S275, 3 mm).

concrete is reduced by 77 %, 87 %, and 91 %, respectively, for 35 %, 50 % and 75 % rubber replacement. This reduction is quite massive and proves rubberised concrete as an inefficient composite, in its unconfined state.

### 3.3. Failure mode for confined specimens

As expected, using CFS for confining RuC is doubly beneficial due to improving both strength properties of RuC and the local buckling resistance of CFS through the restraining effect of the infill. CFS structures are prone to local buckling of their thin-walled sections. The strength of RuC is much lower than that of conventional concrete. Confinement by CFS casings significantly improves that strength. Infilling RuC to CFS sections improves strength of RuC and local-buckling-resistance of CFS, resulting ductile composite elements (RuC-CFS). The composite RuC-CFS sections (in this case RuSCC-CFS) can, therefore, be used for development of a new high-performance framed structural system for multi-storey construction. That structural system has been studied by Bagheri Sabbagh et al. [2,3]. The optimised mix

design of RuSCC and the section properties of CFS determined in this study was used for large-scale cyclic loading tests on the composite RuSCC-CFS structures in the above-mentioned research.

Observations in this research show that confined RuC specimens exhibit a very ductile behaviour (see Fig. 13(a)). A large displacement was measured in the softening regime beyond peak load for the confined specimens. Due to the elastic behaviour of rubber aggregates, for some specimens it was observed that the RuSCC infill bounces back after unloading and gets out of the steel jacket (see Fig. 13(b)). Use of self-drill screws as shear studs in some specimens, although did not alter the failure load significantly, did prevent bouncing back of the RuSCC infill after unloading, as shown in Fig. 13(c).

Fig. 14 compares the failure load for confined RuSCC50%, with and without shear studs. The difference between the load capacity of the two specimens is not significant.

### 3.4. Load-Displacement behaviour for confined specimens

Structural Steel (S275) and Mild Steel (MS) was used for casing, with

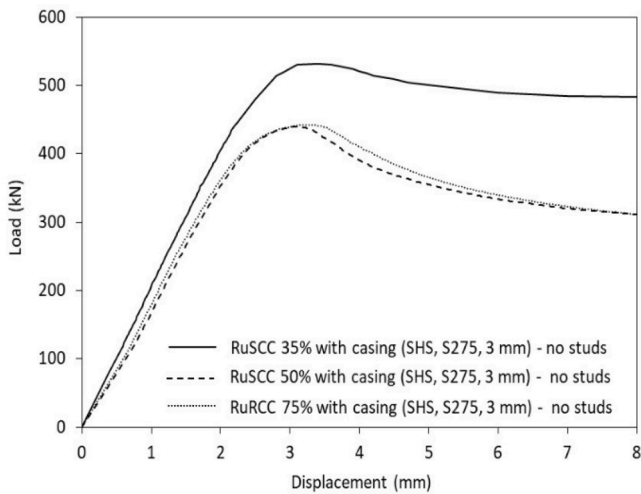


Fig. 20. Comparing the load–displacement behaviour of RuSCC35%, RuSCC50%, and RuRCC75% confined with 3 mm Structural Steel casing (SHS, S275, 3 mm).

Hollow Square Section (SHS) and Hollow Circular Sections (CHS). A thickness of 3 mm was used for S275, and two thicknesses were used for MS (1.6 mm and 3.2 mm).

The hollow casings were first tested under compressive load without any infill. The normalised loads displacement curves were compared in Fig. 15 (the loads on the vertical axes were divided by cross-sectional area of each casing). This comparison shows that the hollow (no infill) steel profiles with a higher thickness (3 mm and 3.2 mm) behave more efficiently and display a higher failure load per cross-sectional area, as well as a higher energy absorption capacity (the area under the curve)

compared to the smaller-thickness profile (1.6 mm) (see Fig. 15). This can be attributed to premature local buckling of the thin-wall profile.

To compare the restraining effect of RuC infill on preventing premature local buckling and improving the efficiency of steel casings, comparison was made between the normalised load–displacement curves for the hollow casings and the casings infilled with RuSCC50%. Fig. 16 shows the results for three types of casings: (SHS, S275, 3 mm), (CHS, MS, 3.2 mm), and (CHS, MS, 1.6 mm).

This comparison displays a higher failure load per cross-sectional area of casing for the composite with Structural Steel, square section and 3 mm thickness of casing (SHS, 275, 3 mm) than the ones with Mild Steel (Fig. 16(a)). Improvement in energy absorption (or increase of the area under the curve) is also higher for the former one (Fig. 16(b) compared to 16(c)). Fig. 16(d) shows that the composite action massively improves the failure load and energy absorption capacity for Mild Steel casing with low thickness (1.6 mm). This can be attributed to higher vulnerability of a thin-wall steel section to premature local buckling, and the more efficient restraining effect of the infill on that. This effect is not as much for the casing with double thickness (3.2 mm), made of the same type of steel and the same shape of section (Fig. 16(c)).

Based on the above comparison, the most efficient casing out of the three is Structural Steel section with 3 mm thickness (SHS, S275, 3 mm), having the highest failure load per cross-sectional area of casing (Fig. 16 (a)) as well as a reasonably good improvement in energy absorption capacity (Fig. 16(b)). To find the best composite for structural frame construction, the load–displacement behaviour of the rubberised concrete incorporating 35 %, 50 % and 75 % rubber aggregates and confined with this type of steel casing will be discussed in the following part.

Fig. 17 shows that the composite action of the confined RuSCC35% with Structural Steel casing of 3 mm thickness (SHS, S275, 3 mm) adds 86kN or 19 % to the sum of the ultimate load bearing capacity of the

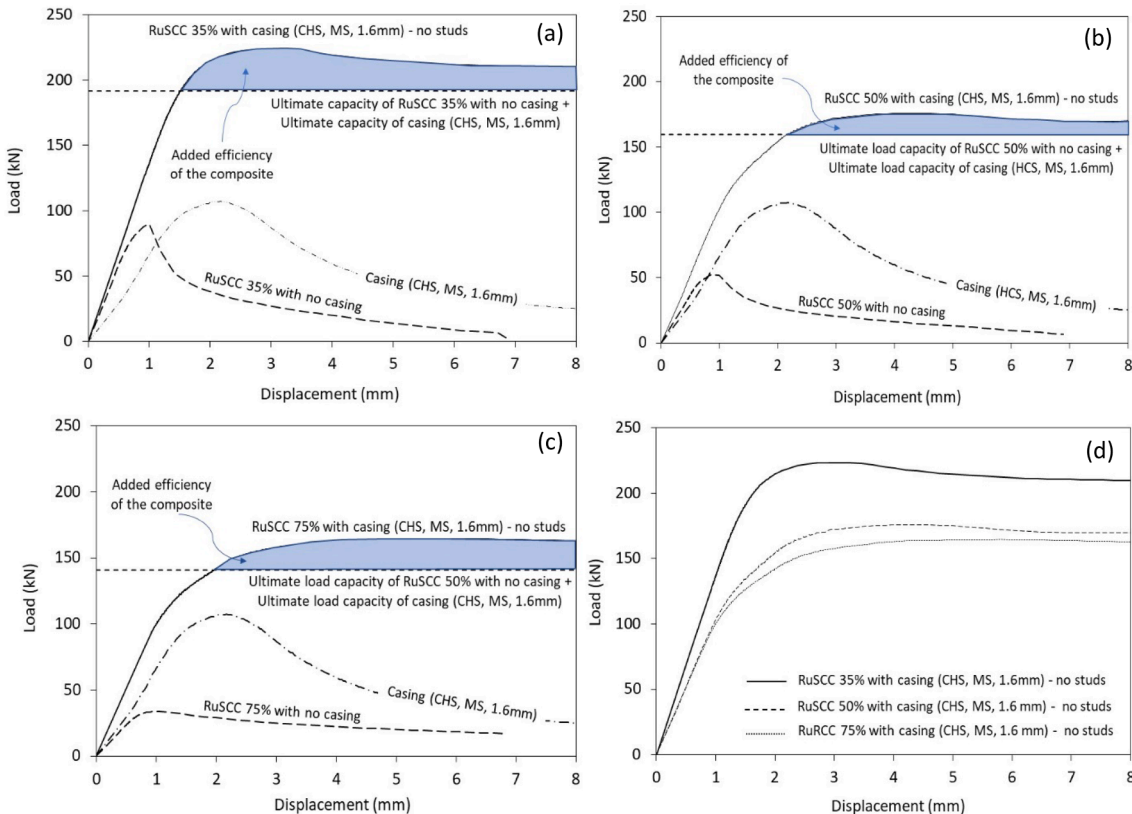


Fig. 21. The composite behaviour of (a) RuSCC35%; (b) RuSCC50%; (c) RuRCC75%, confined with 1.6 mm Mild Steel casing (CHS, MS, 1.6 mm); (d) Comparing the load–displacement behaviour of RuSCC35%, RuSCC50%, and RuRCC75% confined with low thickness Mild Steel casing (CHS, MS, 1.6 mm).

individual constitute materials. It also adds considerably to the energy absorption capacity of the composite. The shaded area in Fig. 17 represents an underestimated amount of this addition.

For RuSCC50% confined with Structural Steel casing of 3 mm thickness (SHS, S275, 3 mm), the composite action only adds 30kN or 7 % above the sum of the ultimate load bearing capacity of the individual constitute materials (Fig. 18). It means that the confined RuSCC35% is a more efficient composite, compared with the confined RuSCC50%.

Due to the difference in the casting technology for RuRCC75% (RCC vs SCC), RuRCC75% confined with Structural Steel casing of 3 mm thickness (SHS, S275, 3 mm) displays a better composite action compared with the confined RuSCC50%. This composite adds 51kN or 13 % above the sum of the ultimate load bearing capacity of the individual constitute materials (Fig. 19).

This comparison shows that RuSCC35% with casing is the most efficient and RuSCC50% with casing is the least efficient composite out of the three, in terms of failure load and energy absorption. Fig. 20 compares the load–displacement behaviour of these three composites.

RCC technology, although is a good solution for pavement and dam construction, cannot be used for infilling steel profiles in structural frames. A high rubber content (say above 50 %) significantly reduces the workability of the rubberised concrete and does not enable satisfactory self-compaction of the infill. Hence, RuRCC50% and RuSCC75% are not suitable for this application, due to their low efficiency and workability, and RuSCC35% will be the remaining option.

To complement the analysis, the comparison is also made for specimens with low thickness Mild Steel casing with circular cross section (CHS, MS, 1.6 mm), for which the effect of infill on increasing the energy absorption capacity proved significant in Fig. 16(d). Fig. 21 shows the results for that comparison and confirms RuSCC35% as the most efficient infill, in terms of increasing the failure load and energy absorption capacity of the composite.

#### 4. Conclusions

Rubberised concrete mixes with high rubber contents were developed by replacing mineral aggregates with various size rubber particles. Composite elements were developed by infilling RuC to steel sections to improve strength of RuC (through jacketing) and local-buckling-resistance of thin-walled steel sections through the restraining effect of the infill. These composite elements were optimized and tested, with the purpose of developing them for structural frames with high energy absorption capacity under extreme loading conditions, while reducing carbon footprint. To enable infilling long steel hollow sections (for beams and columns), the experimental mixes were designed for self-compaction (SCC).

The results show that increasing the rubber contents from 35 % to 50 % (by total volume of the fine and coarse aggregates) decreases the efficiency of the composite. Increasing the rubber contents from 50 % to 75 % decreases the workability of the mix significantly. As a result, the developed mix incorporating 75 % rubber is more suitable for RCC technology rather than SCC.

The mode of failure for RuSCCs was different from what was observed for plain concrete, with ‘Shear’ failure as the dominant mode of failure and ‘Cone and Shear’ and ‘Cone and Split’ failures for some of the specimens. The collapse was very ductile for the confined specimens, and the load was sustained up to a large deformation in the softening regime beyond peak load.

The results proved the confined RuSCC35% with CFS casing (SHS, S275, 3 mm) as the most efficient by adding 86kN or 19 % to the sum of the ultimate load bearing capacity of the individual constitute materials, as well as adding significantly to the energy absorption capacity of the composite. The optimised mix design of RuSCC and the section properties of CFS determined in this study was used for large-scale cyclic loading tests on the composite RuSCC-CFS structures by Bagheri Sabagh et al. [2,3].

For future studies it is recommended to use low carbon cementitious material for more compatibility with a resource efficient composite.

#### Disclaimer

Any opinions, findings, and conclusions or recommendations expressed in this publication are those of the authors and do not necessarily reflect the views of the sponsors and employers.

#### Declaration of Competing Interest

The authors declare that they have no known competing financial interests or personal relationships that could have appeared to influence the work reported in this paper.

#### Acknowledgement

This research was supported by the Royal Academy of Engineering Frontiers of Development Seed Funding scheme on Low-carbon seismic-resistant buildings (FoD2021\4\26).

#### References

- [1] Alsaif A, Garcia R, Figueiredo FP, Neocleous K, Christofe A, Guadagnini M, et al. Fatigue performance of flexible steel fibre reinforced rubberised concrete pavements. *Eng Struct* 2019;193:170–83.
- [2] Bagheri SA, Jafarifar N, Deniz D, Torabian S. Development of composite cold-formed steel-rubberised concrete semi-rigid moment-resisting connections. *Structures* 2022;40:866–79.
- [3] Bagheri SA, Jafarifar N, Davidson P, Ibrahimov K. Experiments on cyclic behaviour of cold-formed steel-rubberised concrete semi-rigid moment-resisting connections. *Eng Struct* 2022.
- [4] Bagheri SA, Petkovski M, Pilakoutas K, Mirghaderi R. Experimental work on cold-formed steel elements for earthquake resilient moment frame buildings. *Eng Struct* 2012;42:371–86.
- [5] Bagheri SA, Petkovski M, Pilakoutas K, Mirghaderi R. Cyclic behaviour of bolted cold-formed steel moment connections: FE modelling including slip. *J Constr Steel Res* 2013;80:100–8.
- [6] British standards Institute. BS EN 12350 Testing Fresh Concrete. BSI British Standards Institute: BS EN; 2010.
- [7] British standards Institute. BS EN 12390 Testing Hardened Concrete. BSI British Standards Institute: BS EN; 2019.
- [8] British standards Institute. BS EN 450–1 Fly ash for concrete. Definition, specifications and conformity criteria. BS EN. BSI British Standards Institute; 2019.
- [9] Dong M, Elchalakani M, Karrech A, Hassanein MF, Xie T, Yang B. Behaviour and design of rubberised concrete filled steel tubes under combined loading conditions. *Thin -Walled Struct* 2019;139:24–38.
- [10] Duarte A, Silva B, Silvestre N, de Brito J, Júlio E, Castro J. Experimental study on short rubberized concrete-filled steel tubes under cyclic loading. *Comp Struct* 2016;136:394–404.
- [11] Elchalakani M, Aly T, Abu-Aisheh E. Mechanical properties of rubberised concrete for road side barriers. *Aust J Civil Eng* 2016;14:1–12.
- [12] Elchalakani M, Hassanein MF, Karrech A, Yang B. Experimental investigation of rubberised concrete-filled double skin square tubular columns under axial compression. *Eng Struct* 2018;171:730–46.
- [13] Han LH, Li W, Bjorhovde R. Developments and advanced applications of concrete-filled steel tubular structures: members. *J Constr Steel Res* 2014;100:211–28.
- [14] Ismail MK, Hassan AAA. Performance of Full-Scale Self-Consolidating Rubberized Concrete Beams in Flexure. *ACI Mater. J* 2016;113:1–6.
- [15] Jafarifar N, Pilakoutas K, Angelakopoulos H, Bennett T. Post-cracking tensile behaviour of steel-fibre-reinforced roller-compacted-concrete for modelling and design purposes. *Mater Constr* 2017;67(326):122–34.
- [16] Jafarifar N, Pilakoutas K, Bennett T. The effect of shrinkage cracks on the loadbearing capacity of steel-fibre-reinforced roller-compacted-concrete pavements. *Mater and Struct* 2016;49(6):2329–47.
- [17] MasterAir 1197 (2020). Air entraining admixture for concrete – Certificate No. 0086-CPD-469071 EN 934-2: T5, BASF.
- [18] MasterGlenium SKY 1966 (2020). High range water reducing admixture for concrete – Certificate No. 0086-CPD-469071 EN 934-2: T3, BASF.
- [19] MasterMatrix SDC 150 (2017). High performance viscosity modifying agent (VMA) for fluid concrete – Certificate No. 0086-CPD-469071 EN 934-2: T13, BASF.
- [20] Mier J.G.M. (2014). Failure of concrete under uniaxial compression: An overview, *Fracture Mechanics of Concrete Structures*, Proceeding FEAMCOS-3.
- [21] Moustafa A, ElGawady MA. Strain rate effect on properties of rubberized concrete confined with glass fiber reinforced polymers. *J Comp Constr* 2016;20(5).
- [22] Parastesh H, Hajirasouliha I, Taji H, Bagheri SA. Shape optimization of cold-formed steel beam-columns with practical and manufacturing constraints. *J Constr Steel Res* 2019;155:249–59.
- [23] Raffoul S, Garcia R, Pilakoutas K, Guadagnini M, Flores Medina N. Optimisation of rubberised concrete with high rubber content: An experimental investigation. *Constr and Build Mater* 2016;124:391–404.

- [24] Raffoul S, Garcia R, Escolano-Margarit D, Guadagnini M, Hajirasouliha I, Pilakoutas K. Behaviour of unconfined and FRP-confined rubberised concrete in axial compression. *Constr Build Mater* 2017;147:388–97.
- [25] Silva A, Jiang Y, Castro JM, Silvestre N, Monteiro R. Monotonic and cyclic flexural behaviour of square/rectangular rubberised concrete-filled steel tubes. *J Constr Steel Res* 2017;139:385–96.
- [26] Shahini M, Bagheri SA, Davidson P, Mirghaderi R. Development of cold-formed steel moment-resisting connections with bolting friction-slip mechanism for seismic applications. *Thin-Walled Struct* 2019;141:217–31.
- [27] Youssef O, ElGawady MA, Mills JE, Ma X. An experimental investigation of crumb rubber concrete confined by fibre reinforced polymer tubes. *Constr and Build Mater* 2014;53:522–32.